DOI: 10.1595/147106704X1603

Ethanol Reactions over the Surfaces of Noble Metal/Cerium Oxide Catalysts

By H. Idriss

The University of Auckland, Department of Chemistry, Auckland, New Zealand; E-mail: h.idriss@auckland.ac.nz

This review focuses on the reactions of ethanol on the surfaces of platinum, palladium, rhodium and gold supported on ceria (of size 10–20 nm). The bimetallic compounds: Pt-Rh, Rh-Au, Rh-Pd, and Pt-Pd were also investigated. Initially this work was aimed at understanding the roles of the different components of automobile catalytic converters on the reactions of ethanol, which is used as a fuel additive. Some of the catalysts that showed high activity for ethanol oxidation were also investigated for hydrogen production. The addition of any of the above metals to CeO_2 was found to suppress the oxidation of ethanol to acetates at room temperature, as there are fewer surface oxygen atoms available to oxidise the ethanol (the remaining oxygen atoms did not produce efficient oxidation). Ethanol dehydrogenation to acetaldehyde was facilitated by the presence of Pt or Pd; at higher temperatures the acetaldehyde condensed to other organic compounds, such as crotonaldehyde. By contrast, in the presence of Rh only traces of acetaldehyde or other organic compounds were seen on the surface, and detectable amounts of CO were found upon ethanol adsorption at room temperature. This indicates the powerful nature of Rh in breaking the carbon-carbon bond in ethanol. The effects of prior reduction were also investigated and clear differences were seen: for example, a shift in reaction selectivity is observed for the bimetallic Rh-containing catalysts. Methane was the dominant hydrocarbon on the reduced catalysts while acetaldehyde was the main product for the non-reduced ones. Hydrogen formation was monitored during steady state ethanol oxidation and Pt-Rh and Rh-Au were found to be the most active catalysts.

Man-made chemicals affect our health and environment through the air, water and soil. Hence seeking suitable, safer alternative chemicals and particularly fuels to replace conventional ones is an ongoing objective. There are several candidates for alternative fuels that can be derived from non-crude oil resources. These include natural gas, liquid petroleum gas (LPG), propane, methanol, ethanol, and hydrogen. Table I characterises various current and alternative fuels (1(a)).

Ethanol as a Source of Hydrogen

Ethanol is an interesting alternative for replacing gasoline as a motor fuel. Ethanol production from sugar- or starch-containing crops is an industrially well-established technique that has been used for many years. Ethanol could indirectly reduce net carbon dioxide emissions from vehicles when used as a 95% blend with gasoline for light-duty vehicles. This is due to the consumption of carbon dioxide by crops used as feedstock for the production of ethanol fuel. Sulfur oxide emissions would also be lowered (by 60 to 80%). Volatile organic compound emissions would be 13 to 15% lower than those of reformulated gasoline (1(b)). Although ethanol is considered to be an attractive replacement fuel, with quite low emissions of complex hydrocarbons, its partial oxidation to acetaldehyde (a potential carcinogen) poses a threat. Hence, the problem of effectively controlling the emissions caused by ethanol oxidation along with the desired conversion requires better understanding.

There are four basic methods for hydrogen production: water electrolysis, a gasification reaction using coal or coke as the feedstock, a partial oxidation reaction using heavy or residual oil as the feedstock, and steam reforming using various

Table I

Characteristics of Various Fuels

Fuel	LHV, BTU/lbm	A/F
Gasoline	18,341	14.6
Light diesel	18,574	14.5
Methane	21,459	17.2
Natural gas	19,257	16.2
LPG	19,757	15.8
Propane	19,879	15.7
Methanol	8,538	6.5
Ethanol	11,546	9.0
Hydrogen	51,352	34.3

LHV (Lower heating value) is used when product-containing water is in its vapour form. The unit of LHV is British Thermal Unit (BTU) per pound mass (lbm).
A/F (Air to Fuel ratio) represents the amount of air required for complete combustion of fuel.
Heating value (HV) is defined as the amount of energy released when a fuel is burned completely in a steady flow process (Adapted from 1(a))

kinds of hydrocarbons as the feedstock. Currently steam reforming is the most important process for hydrogen manufacture; steam reforming of natural gas accounts for almost 50% of the world feedstock for hydrogen (1(c)):

Water electrolysis: $2H_2O \rightarrow 2H_2 + O_2$ (i)

Coal gasification: $CH_{0.8} + 0.6H_2O + 0.7O_2 \rightarrow CO_2 + H_2$ (ii)

Partial oxidation: $CH_{1.8} + H_2O + 0.5O_2 \rightarrow CO_2 + 1.9H_2$ (iii)

Steam reforming: $CH_4 + 2H_2O \rightarrow CO_2 + 4H_2$ (iv)

Much work has been devoted to producing H_2 from ethanol, either by steam reforming or partial oxidation. Fundamental studies of ethanol reactions on metals and oxides, examining the relationships between surface properties (structure, surface defects, etc.) and the reaction yields, have helped to further our understanding of the various processes.

Ethanol Reactions on Surfaces

The ethanol molecule contains two carbon atoms. It can be split at several bonds, see Scheme I. Depending on the type of interaction with the surface of a solid material, the nature of the solid, and the diverse reaction conditions, one may be able to orient the reaction into desired product(s).

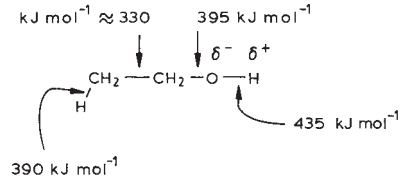

Scheme I
Approximate bond energies for ethanol (2)

The different reactions occurring with ethanol on metal and metal oxide surfaces so far observed are summarised in Scheme II. The reaction can be shifted from CO to CO_2 and from H_2 to H_2O, depending on the ethanol:oxygen ratio. Thus, the balance is not simple and the role of the catalyst is crucial. As the main objective is to find ways to obtain H_2 and CO_2, the catalyst must be active for the water gas shift reaction and for the direct oxidation of CO to CO_2, Equation (xiii) and Figure 1.

The Interaction of Ethanol with CeO_2 and M/CeO_2

The desired catalyst should not be poisoned by CO at the reaction temperature, should allow for a fast O transfer (from the bulk to surface), should allow for fast rejuvenation of the surface oxygen

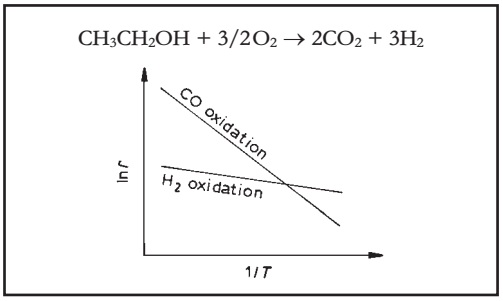

Fig. 1 Schematic of two activated processes: CO oxidation to CO_2 and H_2 oxidation to H_2O. The catalyst chosen would depend on the process temperature. Here, H_2 oxidation has low activation energy while CO to CO_2 has high activation energy. In these conditions increasing the reaction temperature would favour CO to CO_2 and not H_2O formation

$CH_3CH_2OH\,(g) \rightarrow CH_3CH_2O\,(a) + H\,(a)$	(v)	on most oxide surfaces and some metals, such as Pd (3), Ni (4), and Rh (5)
$CH_3CH_2O\,(a) \rightarrow CH_3CHO\,(g) + H\,(a)$	(vi(a))	ΔH_r ((v) + (vi(a)) = 111.5 kJ mol^{-1} on large numbers of oxides (6) and some metals (3)
$CH_3CH_2O\,(a) \rightarrow CH_2CH_2\,(g) + OH\,(a)$	(vi(b))	ΔH_r ((v) + (vi(b)) = 88.4 kJ mol^{-1} on some oxides, usually acidic (7) or in sub-stoichiometric form (8, 9)
$CH_3CH_2O\,(a) \rightarrow CH_2CH_2O\,(a) + H\,(a)$	(vi(c))	on Rh (10, 11)
$CH_3CHO\,(g) + O\,(s) \rightarrow CH_3COO\,(a) + H\,(a)$	(vii)	mainly on basic oxides, such as CeO_2 (12) and ZnO (13)
$2CH_3COO\,(a) \rightarrow CH_3C(O)CH_3 + CO_2 + O\,(a)$	(viii)	ΔH_r (acetic acid (g) to acetone, CO_2 and water) = 13 kJ mol^{-1}; on stoichiometric oxides such as TiO_2 (14), CeO_2 (12) and Fe_2O_3 (15)
$CH_3CHO\,(g) \rightarrow CH_4\,(g) + CO\,(g)$	(ix)	ΔH_r = –18.7 kJ mol^{-1}; mainly on metals (16)
$2CH_3CHO\,(g) \rightarrow CH_3CH{=}CHCHO\,(g) + H_2O\,(g)$	(x)	ΔH_r = –10.3 kJ mol^{-1}; on stoichiometric oxides such as TiO_2 (14), CeO_2 (17), and MgO (18)
$2CH_3CHO\,(g) + 2V_o \rightarrow CH_3CH{=}CHCH_3\,(g) + 2O\,(a)$	(xi)	ΔH_r (acetaldehyde to *trans*-butene and O_2) = 321 kJ mol^{-1}; V_o is oxygen vacancy; on TiO_{2-x} (14) and UO_2 (19)
$3CH_3CHO\,(g) \rightarrow C_6H_6\,(g) + 3H_2O\,(g)$	(xii)	ΔH_r = –144.2 kJ mol^{-1}; on Pt/CeO_2 (20) and UO_{2-x} (21)
$CH_3CH_2OH + 1.5O_2 \rightarrow 2CO_2 + 3H_2$	(xiii)	ΔH_r = –551 kJ mol^{-1}

The elementary steps of Reaction (xiii) can be written as follows (xiii(a)–xiii(d):

$CH_3CH_2OH + 0.5O_2 \rightarrow CH_3CHO + H_2O$	(xii(a))	ΔH_r = –172.9 kJ mol^{-1}
$CH_3CHO \rightarrow CH_4 + CO$	(xiii(b))	ΔH_r = –18.7 kJ mol^{-1}
$CH_4 + H_2O \rightarrow CO + 3H_2$	(xiii(c))	ΔH_r = 205.7 kJ mol^{-1}
$2CO + O_2 \rightarrow 2CO_2$	(xiii(d))	ΔH_r = –566 kJ mol^{-1}

Methane reforming (xiii(c)) and CO oxidation (xiii(d)) may also be interchanged with methane oxidation (xiii(c')) and the water gas-shift reaction (xiii(d')):

$(CH_4 + O_2 \rightarrow 2H_2 + CO_2)$	(xiii(c'))	ΔH_r = –319.1 kJ mol^{-1})
$(CO + H_2O \rightarrow H_2 + CO_2)$	(xiii(d'))	ΔH_r = –41.2 kJ mol^{-1})

Scheme II
Summary of reactions occurring with ethanol on the surfaces of metals and metal oxides
(a) = adsorbed; (g) = gas phase; adsorption and desorption reactions are omitted for simplicity

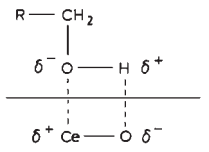

Scheme III
Interaction of an alcohol molecule with the surface of CeO_2 leading to dissociation of the O-H bond

defects (Mars van Krevelen mechanism (22)) and should contain metals that are capable of oxidation/reduction cycles with minimum deactivation. Catalysis by noble metals is usually achieved via the high dispersion of low loading metal(s) (less than one atomic per cent) on an appropriate support. The supports are usually of relatively inexpensive oxide, such as alumina, silica or titania.

Indeed, automobile catalytic converters have now been used for almost three decades and are formed of highly dispersed metals on ceria (CeO_2). Ceria has the fluorite structure (a relatively open structure allowing for a facile oxygen diffusion). It is an ionic oxide of basic character and can be made with high surface area and of nano-dimension particulates. These catalysts (or a variant of

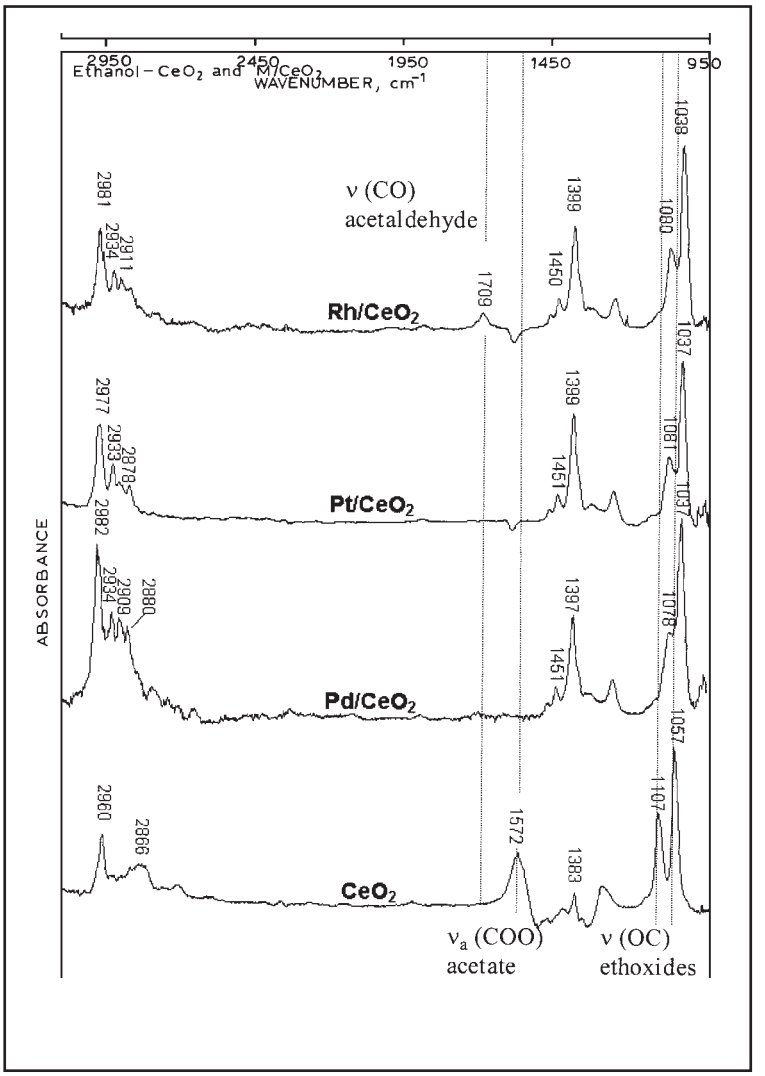

Fig. 2 IR spectra collected upon adsorption of ethanol at 300 K on CeO_2, Pd/CeO_2, Pt/CeO_2 and Rh/CeO_2. Note the presence of acetate species (ν_a = 1572 cm^{-1}) on CeO_2 and their absence on all the other catalysts. Note also the presence of acetaldehyde on Rh/CeO_2 (ν(CO) at 1709 cm^{-1})

them), as will be shown here, can be used for hydrogen production.

The interaction of a polar molecule such as ethanol with the CeO_2 surface would be favoured through the dipole-dipole type as shown in Scheme III. This type of interaction is more known as an acid-base interaction, where the H atom of the acid (in this case ethanol) interacts with one surface O^{2-} (the base). Simultaneously, the Ce^{4+} site (acting as Lewis acid) interacts with the O (2p) orbitals of the oxygen of the adsorbed ethanol molecule. As a result, ethoxide and surface hydroxyl species are formed. Figure 2 shows IR spectra following adsorption of ethanol on the CeO_2 and M/CeO_2 (M = Rh, Pt and Pd) (20, 23, 24). The formation of ethoxides can be seen (two modes of these species are most likely present on CeO_2: monodentate at 1107 cm^{-1}, and bidentate at 1057 cm^{-1}).

CeO_2 is made by precipitation from $Ce(NO_3)_3.6H_2O$ solution by addition of ammonia with stirring at 373 K (pH = 8–8.5). After filtration, washing and drying (at 373 K) calcination was conducted at 773 K for 4 hours under airflow. Metals were deposited on CeO_2 by impregnation from their salts ($RhCl_3.3H_2O$, $PtCl_4$, $PdCl_2$ and $HAuCl_4$) as detailed in (24) and (29).

Three main differences occur in the presence of Pt, Pd or Rh metals (the 'as prepared' metals are actually in oxide form (see (20, 22, 23, 28) for more details on catalyst characterisation):

[1] The two bands (at 1107 and 1057 cm^{-1}) associated to two modes of adsorption for ethoxides have shifted to lower wavenumbers and in addition the first band has become far more pronounced. This is not only due to reduction of CeO_2 because of the presence of the metal (see below) but might also occur due to a direct interaction with the metal particles, see Figure 3.

[2] Acetate species are not observed; as shown below this is due to a partial reduction of the CeO_2 surface.

[3] Bands due to adsorbed acetaldehyde species in η^1(O) configuration are seen. Adsorption of ethanol on H_2-reduced CeO_2 has also been studied and Figure 10 in (23) shows the absence of acetate species due to depletion of surface oxygen.

Extent of CeO_2 Reduction Due to Presence of Noble Metal and CO_2/CO Values

The extent of the reduction of CeO_2 is not constant. It depends on the amount of metal present and also on its nature. One can obtain information from XPS analyses of the O(1s) to Ce(3d) ratios of the 'as prepared' metal containing catalysts. A complementary way of seeing the effect of the reduction is to analyse the CO_2:CO ratio during ethanol temperature programmed desorption (TPD). This is because any CO_2 formed during the ethanol decomposition would contain one oxygen atom from the lattice.

Figure 4 shows a plot of CO_2/CO as a function of the extent of reduction due to the presence of the metal(s). The extent of the reduction is defined as: ΔO/at.% M; where $\Delta O = 2 - x$; 2 is taken because the ratio O to Ce is ideally = 2 (although usually slightly more than 2 on the surface), see Table II for more details. Thus, it is a gauge of any deviation from stoichiometry normalised to the amount of metal. In all metals x is positive

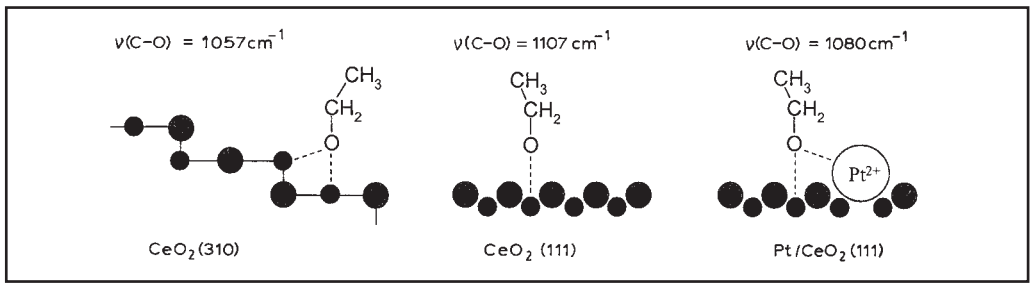

Fig. 3 Schematic representation of the modes of ethoxide species on CeO_2 and in the presence of Pt ions. The presence of stepped surfaces of CeO_2 (such as the 310) makes a bidentate configuration of ethoxide species possible

Table II

A: Effect of Metal Addition on the Reduction of CeO_2, as Determined from the Surface (plus near surface) O to Ce Atomic Ratios

Catalyst	at.% M	O(1s)/Ce(3d) = *x*	ΔO = 2 – *x*	ΔO/at.% M
Pd/CeO_2	0.25	1.76	0.24	0.96
Pt/CeO_2	0.26	1.59	0.41	1.58
Rh/CeO_2	0.17	1.91	0.09	0.53
Au/CeO_2	0.19	2.32	–0.32	–1.68
$Pt\text{-}Pd/CeO_2$	Pt = 0.38; Pd = 0.45	1.51	0.49	0.59
$Au\text{-}Rh/CeO_2$	Au = 0.27; Rh = 0.57	1.49	0.51	0.61
$Pt\text{-}Rh/CeO_2$	Pt = 0.21; Rh = 0.21	1.66	0.34	0.81

B: State of Metal Ions on CeO_2 in the 'As Prepared' Catalysts

Catalyst	Binding Energy, eV, XPS	Assignment
Pd/CeO_2	$Pd(3d_{5/2})$ = 336.5	PdO
Pt/CeO_2	$Pt(4f_{7/2})$ = 74.0	PtO
Rh/CeO_2	$Rh(3d_{5/2})$ = 309.5	RhO_2
Au/CeO_2	$Au(4f_{7/2})$ = 85.6	Au_2O_3
$Pt\text{-}Pd/CeO_2$	$Pd(3d_{5/2})$ = 337.5; $Pt(4f_{7/2})$ = 73.0	
$Au\text{-}Rh/CeO_2$	$Rh(3d_{5/2})$ = 308.7; $Au(4f_{7/2})$ = 85.5	
$Pt\text{-}Rh/CeO_2$	$Rh(3d_{5/2})$ = 309.5; $Pt(4f_{7/2})$ = 73.0	

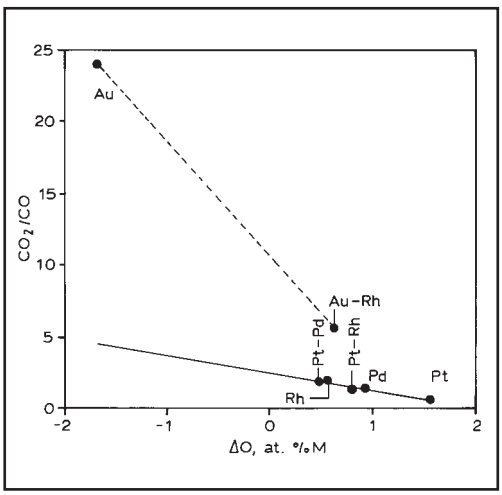

Fig. 4 Plot of CO_2 to CO peak area ratios computed from TPD of ethanol, and the extent of surface reduction (defined in the text). Au/CeO_2 and $Rh\text{-}Au/CeO_2$ catalysts deviate from the linearity observed for the other catalysts.
ΔO = 2 – x; x = O(1s)/Ce(3d)

(decreasing ΔO) with the exception of Au. There are two main features that can be seen in Figure 4:

- First, there is a linear relationship between CO_2/CO and the extent of reduction of CeO_2 for a series containing Rh, Pt, and Pd, as well as for Pt-Pd and Pt-Rh.
- Second, there is a deviation by Au-containing catalysts from this linearity. Thus, based on these 'stoichiometric reaction' results, if one wants to decompose ethanol into CO_2 with high selectivity Au is a far better choice.

CO Adsorption at 90 K, a Molecular Probe

CO adsorption at low temperatures has often been used as a way of characterising specific adsorption sites on metals and metal oxides. It is important to emphasise that the metals being discussed here, are actually in an oxidised form – as indicated before. Figure 5 shows the irreversible adsorption of CO at 90 K on CeO_2 alone and

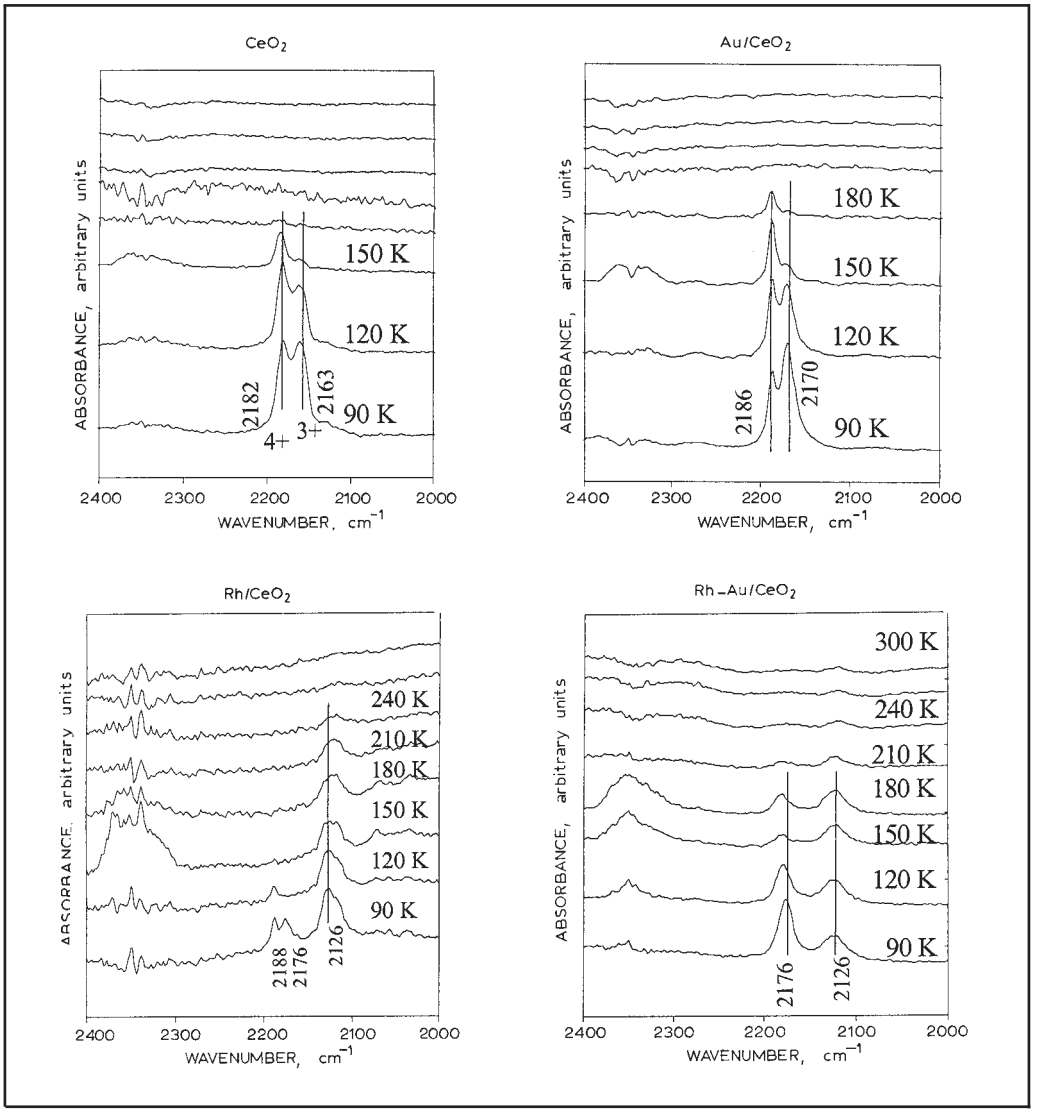

Fig. 5 Irreversible CO adsorption after saturation at 90 K over CeO_2, Au/CeO_2, Rh/CeO_2 and $Rh\text{-}Au/CeO_2$. The catalysts were heated at the indicated temperatures after CO adsorption at 90 K, then quenched back to 90 K for further data collection

when impregnated with metals, and the following points should be noted:

[a] The presence of both Ce^{4+} and Ce^{3+} on the surface of CeO_2 are clearly seen by CO adsorption as the probe. CO is adsorbed via an electrostatic interaction that disappears by 150 K.

[b] In the presence of Rh ions, bands characteristic of linear CO are seen (note the relative stability of these bands compared to those of CO on CeO_2 alone).

[c] The presence of both Rh and Au ions together appear masking the CO electrostatic adsorption on Ce^{4+} ions.

Oxidation/Reduction Reactions

In a system where oxidation reactions occur (such as ethanol to CO_2) the state of the metal may oscillate between oxidation and reduction. It is thus worth studying the effect of prior reduction of the metal on the outcome of the ethanol

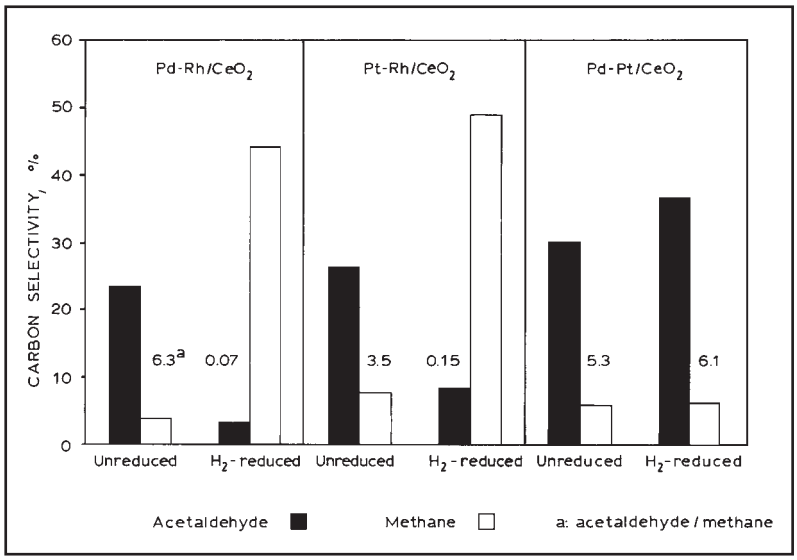

Fig. 6 Switch in reaction selectivity between reduced and non-reduced M/CeO_2 catalysts prior to ethanol oxidation. The presence of Rh shifts the reaction products from acetaldehyde to methane when the catalyst has been reduced with H_2

decomposition. There is a clear shift in the reaction selectivity as shown by representative data below. The 'as prepared' Pd/CeO_2, Pt/CeO_2, Au/CeO_2 and Rh/CeO_2 show the formation of acetaldehyde. Acetaldehyde made by dehydrogenation (in the presence as well as the absence of oxygen) of ethanol has been seen by IR spectroscopy (as an adsorbed species), during TPD and in steady state catalytic conditions. The main point is that prior reduction shifts the Rh/CeO_2 catalysts from CH_3CHO directly to CO formation (23).

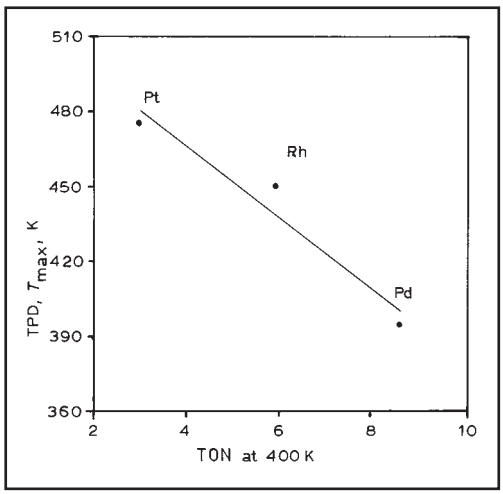

Fig. 7 Correlation between TPD peak desorption temperature and the TON for ethanol oxidation. The TON is defined as the number of molecules of ethanol converted per surface M atom (as computed from the corrected XPS signal) per second. The higher the TON the lower is the desorption temperature of acetaldehyde

In the absence of a good hydrogenating catalyst most of the CO desorbs. The addition of a second metal (Pt or Pd) is dramatic. Figure 6 shows the selectivity shifts from acetaldehyde, on the unreduced bimetallic Rh-containing catalysts, to methane on the reduced catalysts. In the absence of Rh, acetaldehyde is only marginally affected by the reduction process. This can be interpreted as follows: Rh is an efficient catalyst for carbon-carbon bond dissociation and this is shown by the presence of adsorbed CO, even at low temperature, upon dosing the rhodium surface with ethanol. In the presence of a good hydrogenation catalyst (such as Pd) and upon heating CO is converted to methane.

Comparing TPD to Catalytic Reactions

Good similarity between TPD and catalytic reactions can be seen in Figure 7. The turnover number (TON) determined from the rate of ethanol reaction in steady state catalytic reactions tracks the desorption temperature of acetaldehyde (during ethanol-TPD) for Rh/CeO_2, Pd/CeO_2 and Pt/CeO_2.

Acetaldehyde is weakly adsorbed on the surface and its desorption is reaction limited (as soon as

Table III

A: Product Distribution (in mol%) during Ethanol Reaction [Ethanol]/[O_2] = 2/3; [Catalyst] = 50 mg; F = 200 ml min^{-1} over Au/CeO_2 at the Indicated Temperatures

	473 K	573 K	673 K	773 K	873 K	973 K	1073 K
CH_3CHO	56.44	25.52	9.88	6.46	5.01	0.1	0.07
CH_4	7.53	5.67	18.50	7.26	8.81	24.77	24.65
$CH_3C(O)CH_3$	–	3.18	6.69	36.98	26.82	0.75	–
CO	–	8.25	10.23	16.80	22.02	31.12	31.34
CO_2	31.91	55.54	52.32	27.85	32.52	34.14	35.01
CO/CO_2	0	0.15	0.20	0.60	0.68	0.91	0.90
H_2	4.12	1.86	2.37	4.65	4.81	9.11	8.93

B: Product Distribution (in mol%) during Ethanol Reaction [Ethanol]/[O_2] = 2/3; [Catalyst] = 50 mg; F = 200 ml min^{-1} over Rh-Au/CeO_2 at the Indicated Temperatures

	473 K	573 K	673 K	773 K	873 K	973 K	1073 K
CH_3CHO	66.60	0.74	0.04	0.03	0.04	0.03	0.01
CH_4	17.99	19.04	16.95	14.39	11.24	10.97	12.63
$CH_3C(O)CH_3$	–	1.49	0.12	0.23	–	–	–
CO	–	24.34	13.98	15.65	19.70	21.62	23.58
CO_2	–	49.44	56.16	54.62	53.68	52.75	49.00
CO/CO_2		0.49	0.25	0.29	0.37	0.41	0.48
H_2	15.42	4.95	12.74	15.09	15.34	14.63	14.77

C: Product Distribution (in mol%) during Ethanol Reaction [Ethanol]/[O_2] = 2/3; [Catalyst] = 50 mg; F = 200 ml min^{-1} over Pt-Rh/CeO_2 at the Indicated Temperatures

	473 K	573 K	673 K	773 K	873 K	973 K	1073 K
CH_3CHO	48.72	0.97	2.72	0.66	–	–	–
CH_4	10.84	17.71	17.10	15.78	11.98	9.07	9.53
$CH_3C(O)CH_3$	–	–	1.18	2.28	–	–	–
CO	–	15.25	13.33	12.12	12.14	13.06	16.26
CO_2	32.62	61.67	58.31	57.46	58.82	60.26	59.86
CO/CO_2	0.25	0.23	0.21	0.21	0.22	0.27	0.25
H_2	7.82	4.39	7.36	11.69	17.07	17.61	14.35

the H of the CH_2 is abstracted from the ethoxide species acetaldehyde is formed and desorbs). This means that the desorption temperature during TPD contains in large part the activation of the C-H bond of the CH_2 of ethoxides. The higher the desorption temperature of acetaldehyde during TPD the lower is the TON and *vice versa*.

Hydrogen Production

From the above studies it appears that bimetallic catalysts containing Rh are better suited for ethanol decomposition. We have conducted detailed studies of Pt-Rh/CeO_2 and Rh-Au/CeO_2 by IR spectroscopy and TPD and in steady state reaction conditions. Both catalysts are very active for ethanol decomposition. Table III (A to C) summarises most of the steady state reaction data. The reactions ethanol undergoes first proceed via a dehydrogenation of ethanol to acetaldehyde. The faster acetaldehyde is decomposed, the more efficient is the total decomposition (as in a typical consecutive reaction). The addition of Rh dramatically destabilises acetaldehyde and this is probably due not only to further conversion of acetaldehyde to CO and CH_4 but also to a specific direct interaction between Rh and ethoxide species (as an

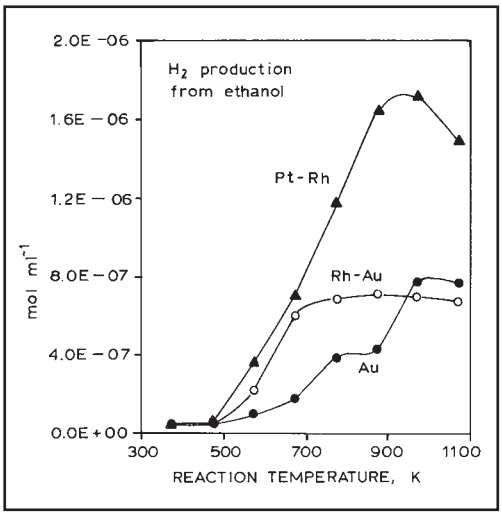

Fig. 8 H_2 production during the catalytic reaction of ethanol on Au/CeO_2, $Rh\text{-}Au/CeO_2$ and $Pt\text{-}Rh/CeO_2$. $[Ethanol]/[O_2] = 2/3$; [Catalyst] = 50 mg; F(ethanol flow) = 200 ml min^{-1}; $[Ethanol]_o = 2.5 \times 10^{-6}$ mol ml^{-1} for Au/CeO_2 and 3.2×10^{-6} mol ml^{-1} for both $Rh\text{-}Au/CeO_2$ and $Pt\text{-}Rh/CeO_2$. All measurements taken under steady state conditions

oxametallacycle) (10, 11). The decomposition of the latter would also give CO and CH_4. Most CO is oxidised to CO_2 at low temperatures. Acetone results as a secondary reaction of acetaldehyde (via acetate species), which explains its disappearance in the presence of Rh. At low temperatures Au/CeO_2 showed the lowest CO to CO_2 ratios but the effect of Au seems to disappear at higher temperatures. Figure 8 shows H_2 production as a function of reaction temperature in steady state conditions. Although $Rh\text{-}Au/CeO_2$ and $Pt\text{-}Rh/CeO_2$ are of comparable activity towards H_2 formation at low temperatures, the latter catalyst is far better above 700 K.

Scheme IV has been constructed from spectroscopic and kinetic data. The addition of Rh metal largely suppressing the dehydrogenation route is most likely due to the formation of a bicoordinated species (via the O and the C ends: oxametallacycle). This five-member oxametallacycle species has not been seen on these catalysts but has been computed (and proposed) by other workers as the most probable species resulting from iodo-ethanol and ethylene oxide molecules on Ag and Rh surfaces (10, 24, 25, 26). Further decomposition of this species will yield CO and CH_4 and/or CH_x depending on the nature of the metal. The high temperature production of H_2 is most likely associated with the oxidative dehydrogenation as well as reforming of CH_4 and CO. There is a great deal still to be learned in this generalised reaction scheme and particularly the role of these metals both in reforming and in the water gas shift reaction (see for example (27–36)).

Conclusions

The complexity of the ethanol reactions on the surfaces of noble metals/cerium oxide catalysts is outlined. Hydrogen production from ethanol is directly related to two main steps. The first involves breaking the carbon-carbon bond, and Rh appears the most suitable compound for this reaction at reasonable operating temperatures. The second involves CO oxidation to CO_2. While finely dispersed Au is a very active catalyst for CO oxidation during TPD, the high temperature requirement for good hydrogen yield in steady state conditions may favour other metals, such as Pt.

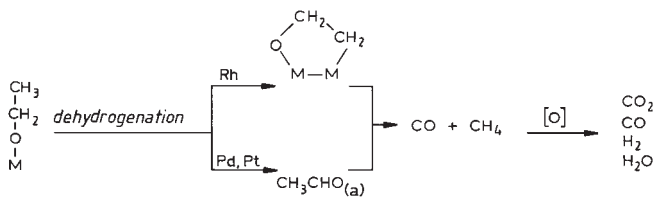

Scheme IV

The difference in the reaction pathways between Rh and Pd and Pt catalysts; (a) for adsorption; [O] for surface oxygen and M for a metal or a Ce ion site

References

1 (a) T. T. Maxwell and J. C. Jones, "Alternative Fuels, Emissions, Economics, and Performance", Society of Automotive Engineers, Warrendale, PA, 1995; (b) M. E. Himmel, W. S. Adney, J. O. Baker, R. Elander, J. D. McMillan, R. A. Nieves, J. J. Sheehan, S. R. Thomas, T. B. Vinzant, and M. Zhang, in: "Fuels and Chemicals from Biomass", eds. B. C. Saha and J. Woodward, ACS Symposium Series 666, American Chemical Society, Washington D.C., 1997, pp. 2–45; (c) "Kirk-Othmer Encyclopedia of Chemical Technology", 4th Edn., Wiley-Interscience, 1992, Vol. 13

2 "Handbook of Chemistry and Physics", 76th edition, Chief Editor D. R. Lide, CRC Press, Boca Raton, 1995–1996

3 J. L. Davis and M. A. Barteau, *Surf. Sci.*, 1990, **235**, 235

4 S. M. Gates, J. N. Russell and J. T. Yates, *Surf. Sci.*, 1986, **171**, 111

5 Z. I. Tian, X. M. Wei, R. S. Zhai, S. Z. Ren, D. B. Liang and L. W. Lin, *Chem. J. Chin. Univ.*, 1997, **18**, 1153

6 H. Idriss and E. G. Seebauer, *J. Mol. Catal. A: Chem.*, 2000, **152**, 201

7 J. Haber, K. Pamin, L. Matachowski, B. Napruszewska and J. Poltowicz, *J. Catal.*, 2002, **207**, 296

8 S. V. Chong, M. A. Barteau and H. Idriss, *Catal. Today*, 2000, **63**, 283

9 B. M. Abu-Zied and A. M. El-Awad, *J. Mol. Catal. A: Chem.*, 2001, **176**, 227

10 M. Mavrikakis, D. J. Doren and M. A. Barteau, *J. Phys. Chem. B*, 1998, **102**, 394

11 N. F. Brown and M. A. Barteau, *Surf. Sci.*, 1993, **298**, 6

12 H. Idriss, C. Diagne, J. P. Hindermann, A. Kiennemann and M. A. Barteau, *J. Catal.*, 1995, **155**, 219

13 J. M. Vohs and M. A. Barteau, *Surf. Sci.*, 1986, **176**, 91

14 K. S. Kim and M. A. Barteau, *J. Catal.*, 1990, **125**, 353

15 E. J. Grootendiorst, R. Pestman, R. M. Koster and V. Ponec, *J. Catal.*, 1994, **148**, 261

16 J. L. Davis and M. A. Barteau, *J. Am. Chem. Soc.*, 1989, **111**, 1782

17 H. Idriss, K. S. Kim and M. A. Barteau. *J. Catal.*, 1993, **139**, 119

18 J. I. Dicosimo, V. K. Diez, M. Xu, E. Iglesia and C. R. Apesteguia, *J. Catal.*, 1998, **178**, 499

19 H. Madhavaram and H. Idriss, *Stud. Surf. Sci. Catal.*, 1997, **110**, 265

20 A. Yee, S. J. Morrison and H. Idriss, *J. Catal.*, 2000, **191**, 30

21 S. V. Chong and H. Idriss, *J. Vac. Sci. Technol. A*, 2001, **19**, 1933

22 P. Mars and D. W. van Krevelen, *Chem. Eng. Sci.,* 1954, **3** (suppl.), 41

23 A. Yee, S. J. Morrison and H. Idriss, *Catal. Today*, 2000, **63**, 327

24 A. Yee, S. J. Morrison and H. Idriss, *J. Catal.*, 1999, **186**, 279

25 M. Mavrikakis and M. A. Barteau, *J. Mol. Catal. A: Chem.*, 1998, **131**, 135

26 S. Linic, H. Piao, K. Adib and M. A. Barteau, *Angew. Chem.,* in press

27 G. S. Jones, M. Mavrikakis, M. A. Barteau and J. M. Vohs, *J. Am. Chem. Soc.*, 1998, **120**, 3196

28 P. Y. Sheng, A. Yee, G. A. Bowmaker and H. Idriss, *J. Catal.*, 2002, **208**, 393

29 P. Y. Sheng, G. A. Bowmaker and H. Idriss, *Appl. Catal. A: Gen.*, 2004, **261**, 171

30 H. He, H. X. Dai, L. H. Ng, K. W. Wong and C. T. Au, *J. Catal.*, 2002, **206**, 1

31 Q. Fu, H. Saltsburg and M. Flytzani-Stephanopoulos, *Science*, 2003, **301**, 935

32 S. Hilaire, X. Wang, T. Luo, R. J. Gorte and J. Wagner, *Appl. Catal. A, Gen.*, 2004, **258,** 271

33 D. Andreeva, *Gold Bull.*, 2002, **35**, (3), 82

34 M. A. Henderson, C. L. Perkins, M. H. Engelhard, S. Thevuthasan and C. H. F. Peden, *Surf. Sci.,* 2003, **526**, 1

35 S. Golunski, R. Rajaram, N. Hodge, G. J. Hutchings and C. J. Kiely, *Catal. Today,* 2002, **72**, 107

36 A. F. Ghenciu, *Curr. Opin. Solid State Mater. Sci.*, 2002, **6**, 389

The Author

Hicham Idriss is an Associate Professor in the Department of Chemistry at the University of Auckland, New Zealand. His research interests include the fundamental and applied study of surface-gas interactions on oxide and metal/oxide surfaces; the design, synthesis and study of new oxide materials of relevance to environmental, petrochemical and electronic applications. Current work involves the total decomposition of ethanol to hydrogen with high yield and low CO production. This includes fundamental studies of Au and Rh (in their metallic and oxidised states) on titania single crystals.

He began his career as a lecturer in the School of Chemistry, University of Strasbourg, France, followed by postdoctoral/research associate work (Department of Chemical Engineering), University of Delaware, U.S.A. After this he was Group Leader, Catalysis and Technology, SABIC, Saudi Arabia; then a Research Associate (Department of Chemical Engineering), University of Illinois, Urbana, IL, U.S.A.

Since 1995 he has been in New Zealand at the University of Auckland.